The mechanism of the formation of boron ineffective zone and its effect on the properties of Ultralow carbon bainitic steels

RONG-IUAN HSIEH, SHYI-CHIN WANG, HORNG-YIH LIOU
Steel and Aluminium Research and Development Department, China Steel Corporation, Taiwan

In the manufacturing of ultralow carbon bainitic (ULCB) steels, boron is an alloying element which is essential to promote the desired bainitic transformation. In order to obtain this hardenability effect, boron must be in solution and it must segregate to the austenite grain boundary and where it decreases the contribution of the boundary's interfacial energy to ferrite nucleation. During the development of ULCB steels in China Steel Corporation, a small boron ineffective zone was found at the centre of steel plates. From electron-probe X-ray microanalysis (EPMA) and boron autoradiograph analysis, it was found that the formation of the boron ineffective zone was due to the centre-line segregation of inclusions which strongly combined with boron and formed a boron-free zone in its vicinity. The microstructure of the boron ineffective zone was a conventional ferrite with a strength which was much lower than that of the surrounding bainite. This resulted in crack separation in the tensile and impact specimens. It was found from a hydrogen-induced-cracking (HIC) test, that the HICs had a propensity to propagate along the boron ineffective zone. From a welding *y*-grooved test, a higher cold-cracking sensitivity at this boron ineffective zone was also found.

1. Introduction

As the exploration and the production of gas and oil have been made in deeper and colder areas, large-diameter pipelines are increasingly required to transport oil and gases through severe environments. In addition, in order to improve the transportation efficiency, large-diameter pipelines operating at higher pressures are desired. As a result, the specification for pipeline steels becomes more and more critical, and it is quite a challenge to steelmakers to manufacture steel plates which are suitable for this application. During the last two decades, with the help of controlled rolling and microalloying technology, a series of ultralow carbon bainitic (ULCB) steels have successfully been developed in the as-rolled condition. Because of their high strength, their high toughness, their good weldability and their superior resistance to hydrogen-induced cracking (HIC), these kinds of steels have been successfully applied not only in the construction of transmission pipelines but also in some other critical applications such as the HY-80 alternative for warship construction and in automobile bumpers and frames [1, 2]. In the manufacturing of ULCB steels, boron must be retained in solid solution, and then it might segregate to the austenite grain boundary and inhibit ferrite formation. Because boron has a strong affinity with nitrogen, it is necessary to fix the nitrogen to protect the boron from the formation of BN. This is usually done by adding small amounts of titanium to form stable TiN particles [3, 4]. Furthermore, it has been reported that if the full effect of boron is to be achieved, the sulphur, oxygen and other impurity levels should be kept as low as possible [5, 6]. However, the mechanism by which impurities affect the behaviour of boron, and its effect on the mechanical properties of steel plates, have never been specified. During the development of ULCB steels in CSC, a small boron ineffective zone was found at the centre of steel plates. The purposes of this study were to investigate the mechanism for the formation of the boron ineffective zone and its effect on the properties of ULCB steels.

2. Experimental procedures

The experimental ULCB steels were prepared from 250 kg vacuum melt heats and cast into 160 mm × 160 mm square ingots. The chemical compositions of the experimental steels are listed in Table I. Basically, these steels were microalloyed with 0.045% Nb and 15 parts per million (p.p.m.) B. As a result of the high Mn content of around 1.8%, the granular bainite structure can be obtained in the as-rolled condition. In order to protect boron from the formation of BN, around 0.02% Ti was added to these steels to fix the nitrogen present by the formation of stable TiN. Before rolling, the steels were reheated at 1150 °C for 2 h. During rolling, the temperature was measured with an optical pyrometer. The final rolling temperature was controlled and varied in the range 760–850 °C.

0022–2461

TABLE I The chemical compositions of experimental steels

C (wt%)	Si (wt%)	Mn (wt%)	P (p.p.m.)	S (p.p.m.)	Al (wt%)	Ti (wt%)	Nb (wt%)	N (p.p.m.)	B (p.p.m)
0.021	0.16	1.80	140	34	0.020	0.020	0.046	28	17

This was achieved by adjusting the slab temperature when the thickness was reduced to two times the final thickness. The rolling reduction per pass was around 20% and the final thickness was varied from 15–35 mm.

In order to analyse the distribution of boron at the boron ineffective zone, which is normally found at the centre of steel plates, the fission-tracking-etching (FTE) method was used. At the same time, electron probe X-ray microanalysis (EPMA) was used to analyse the compositions of the inclusions at the centre of the steel plates. The specimens for the microstructural investigation were mechanically polished and then etched with a 3% nital solution.

A HIC resistance evaluation was performed according to the National Association of Corrosion Engineers (NACE) TM-02-84 standard. Three pieces of specimens (100 mm × 20 mm × full thickness) were sectioned from the longitudinal direction of the steel plates. Samples were ground with emery paper to #320, and then they were immersed in a BP solution which was an artificial-sea-water solution with saturated H_2S. After immmersion for 96 h, each sample was cut into four even pieces to measure the crack-length ratio (CLR), which is defined as the ratio of the total crack length along the width direction to the width of specimen.

A Y-grooved test was conducted according to the Japanese Industrial Standard (JIS) Z 3158 standard to evaluate the cold-cracking sensitivity of the heat-affected zone. The welding heat input was 17 kJ cm^{-1} using an E9016 electrode which had a diameter of 4.0 mm. After welding for 48 h, five specimens were sectioned and polished to observe the initiation and propogation of cold cracking at the heat-affected zone.

3. Results and discussion

Fig. 1 shows a scanning electron microscopy (SEM) micrograph of the as-rolled ULCB steel. It has a typical granular bainite structure and is composed of a bainitic ferrite matrix with small amount of a uniformly distributed second phase. The majority of the second phase is a granular, light-etching phase, which has been identifed as being composed of martensite and austenite [7, 8]. Fig. 2a shows a photograph of a polished and etched specimen sectioned from the transverse direction of as-rolled ULCB steel. A stringer-like abnormal region with darker contrast can be observed in the central portion of the plates. From the microstructural observation, in Fig. 2b, ferrite and pearlite structures were found instead of the normal bainite structure. The measured through-thickness hardness distribution is shown in Fig. 3. It can be found that the hardness of this abnormal stringer-like region is about 20% lower than that of the surrounding sound region. In order to study the reason for the formation of the stringer-like-incomplete-transformation soft region, the distribution of the boron in the central portion of the experimental steel plate was measured using the FTE method. Fig. 4 shows the uneven distribution of boron. In the sound region, the distribution of boron is uniform. However, a stringer of boron-enriched clusters which might be in form of a precipitate is observed in the centre of the plate. Furthermore, a boron-depleted zone can also be found in its vicinity. Fig. 5 shows an optical micrograph at the incomplete-transformation-soft-region where a stringer-like inclusion is surrounded by a ferrite–pearlite structure. It has been reported that, during cooling of cast ingots, excessive segregation of boron to the stringers of large inclusions may occur. When boron segregates into the inclusions, it is unable to dissolve into the steel matrix to perform its function in increasing the hardenability of steels [9, 10]. Fig. 6 shows the element-distribution-analysis result of this stringer-like inclusion using EPMA. It is an oxide inclusion which is mainly composed of manganese and silicon. Enrichment of boron can also be found in this inclusion. On the basis of these analysis results, it is certain that the formation of a stringer-like abnormal soft region with a ferrite–pearlite structure is due to the existence of stringers of (Mn,Si)O oxides in the centre of the plate. The oxide inclusions might extensively absorb boron from the surrounding matrix and therefore remove its ability to promote bainite transformations.

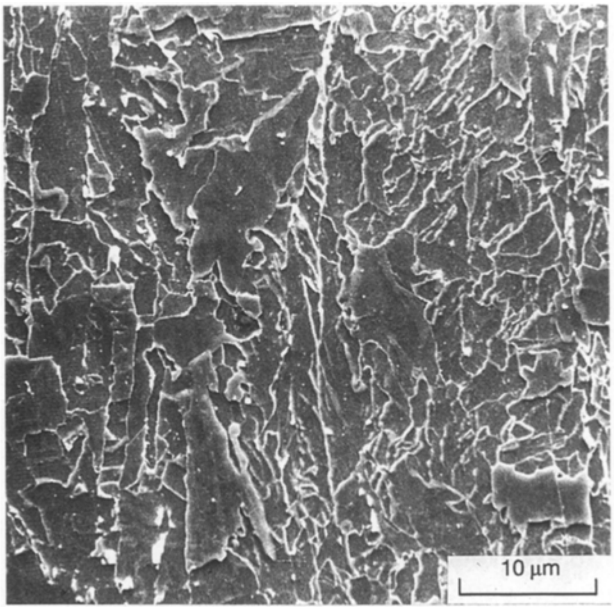

Figure 1 A scanning electron micrograph of ULCB steel in the as-rolled condition.

A systematic analysis of the effect of the boron ineffective zone and the resulting incomplete-transformation soft region on the mechanical properties,

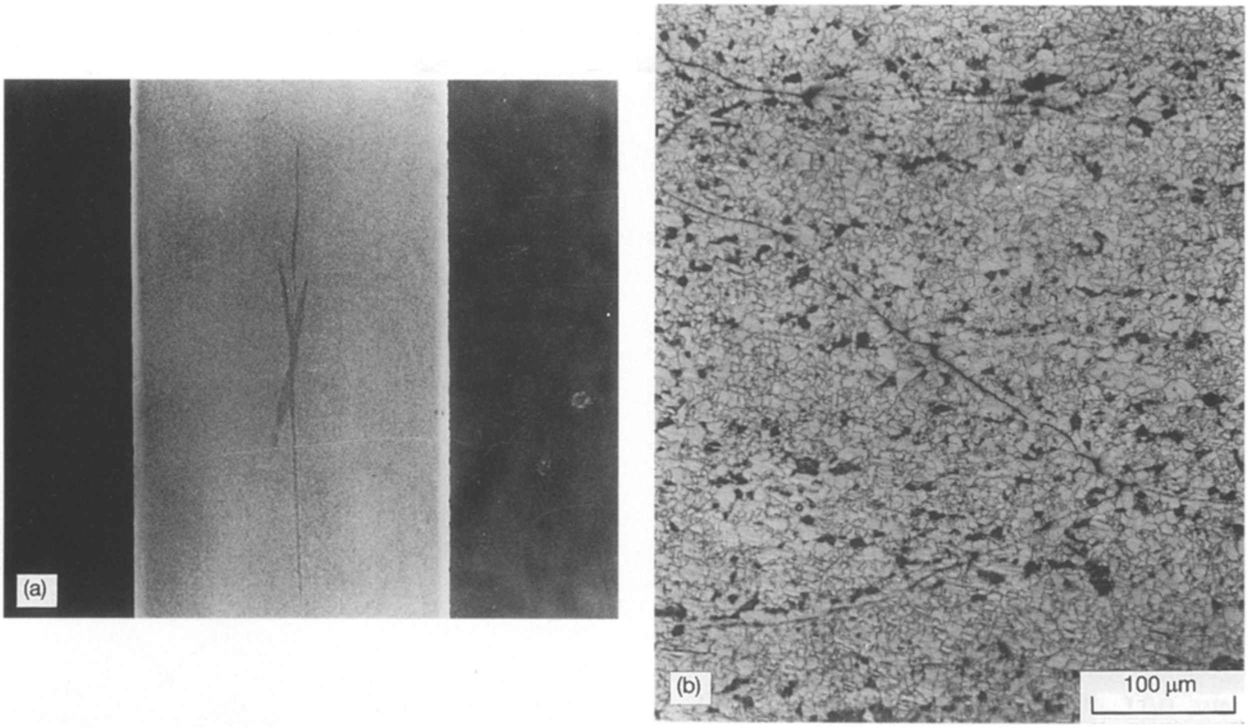

Figure 2 The incomplete transformation zone at the centre line of the ULCB steel: (a) a photograph of a stringer-like abnormal region, and (b) a micrograph of the ferrite and the pearlite structure at the abnormal region.

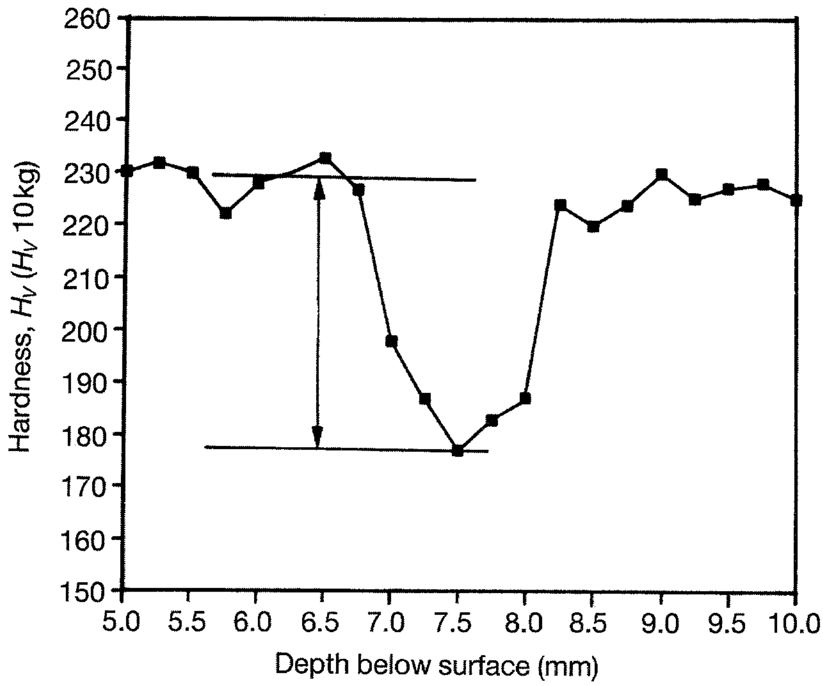

Figure 3 The measured through-thickness hardness distribution showing the relatively softer region at the centre of the plate.

on the HIC resistance and on the cold-cracking sensitivity of the heat-affected zone. These results can be described as follows.

3.1. The occurrence of crack separation in the tensile and charpy specimens

During tensile testing, a short, transverse, tensile stress will be induced when necking occurs. Because this stress acts transversely on the incomplete-trans- formation soft region, all the plastic strain in the short, transverse, direction will be locally concentrated at this relatively softer region. Finally, the locally excessive plastic deformation will result in crack separation of the tensile specimen. Fig. 7a shows photographs of the fractured tensile specimen. The separation along the centre line of the steel plate can clearly be seen. From the microstructural observation shown in Fig. 7b, the

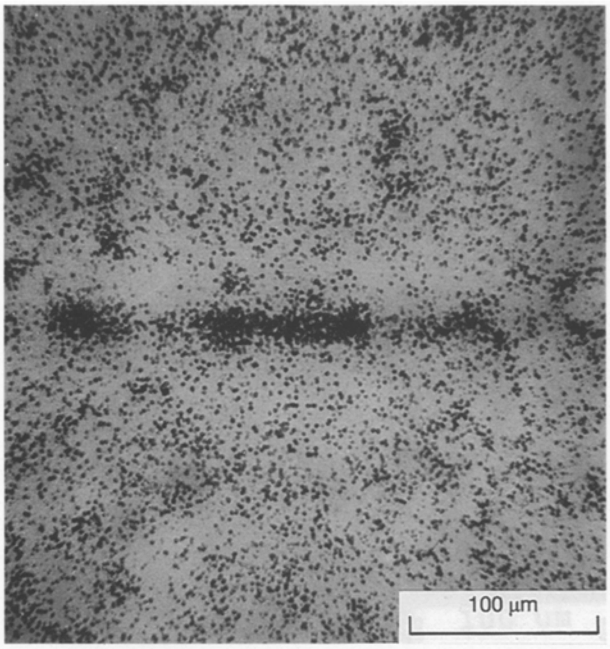

Figure 4 An optical micrograph showing the distribution of boron in the vicinity of the centre line incomplete-transformation zone.

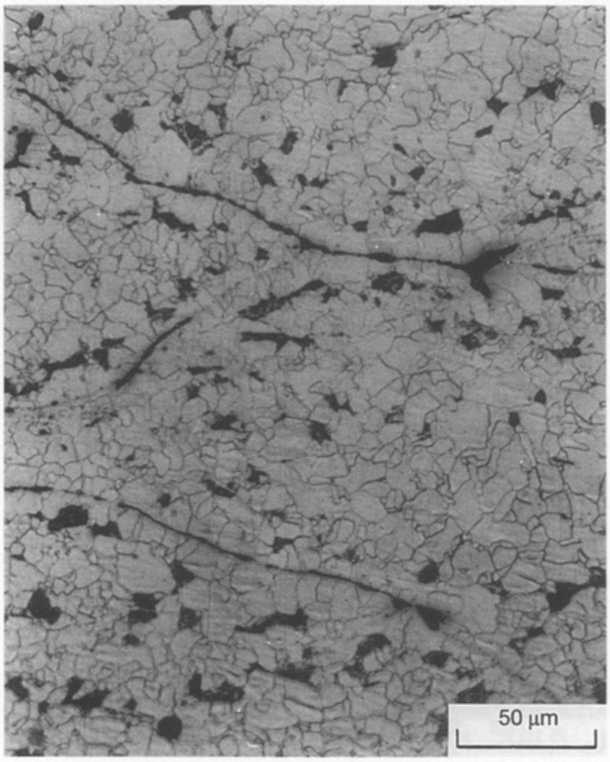

Figure 5 An optical micrograph at the incomplete-transformation zone showing a stringer-like inclusion surrounded by a ferrite and pearlite structure.

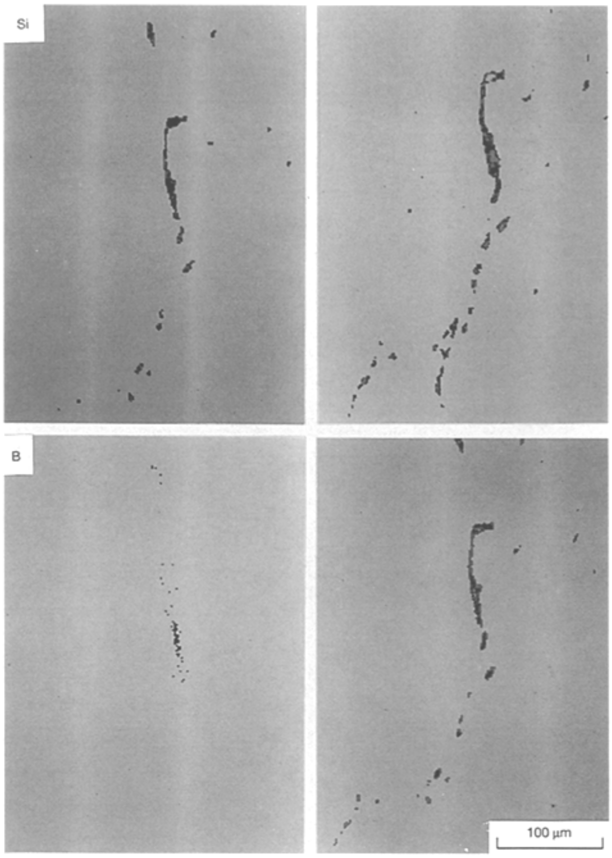

Figure 6 Photographs showing the element-distribution-analysis result for the stringer-like inclusion using EPMA.

separation fracture surface propagates along the incomplete-transformation soft region with the ferrite and pearlite structure. Fig. 7c shows a SEM micrograph of the separated surface; the fracture morphology is characterized by extremely shallow dimples which respond to ductile fracture by plastic deformation in a restricted, shallow, region. The tensile-test results revealed that the occurrence of the separation does not have a critical effect on the strength and toughness of steel plates, but it does have a minor detrimental effect on the elongation. In fact, the separation phenomenon has been found on the conventional HSLA steels because of the crystalline texture developed by severe controlled rolling [11]. The mechanism of the separation is the same in both cases, that is, the fracture stress in the short, transverse, direction of the steel plate is at least 20% lower than that in the transverse or longitudinal direction [12]. However, the reason for the low fracture stress in the thickness direction is different. In this case, the reason for the reduction of the fracture strength in the thickness direction, and the consequent separation, arises from the formation of the incomplete-transformation soft region at the centre of the steel plate. In contrast, in conventionally controlled rolled HSLA steels, the reduction in the fracture stress in the thickness direction originates in the development of the rolling texture.

3.2. Local aggravation of hydrogen-induced cracking (HIC)

It has been found that ULCB steels have a superior HIC resistance to conventional HSLA steels with a ferrite and pearlite structure. This can be attributed to their lower carbon content and their extremely uniformly distributed second phases. As described above, the microstuctures of the boron ineffective zone at the centre of the steel plates are ferrite and pearlite. Moreover, the pearlite band, which is a good route for HIC propagation [13, 14], is very pronounced. It is

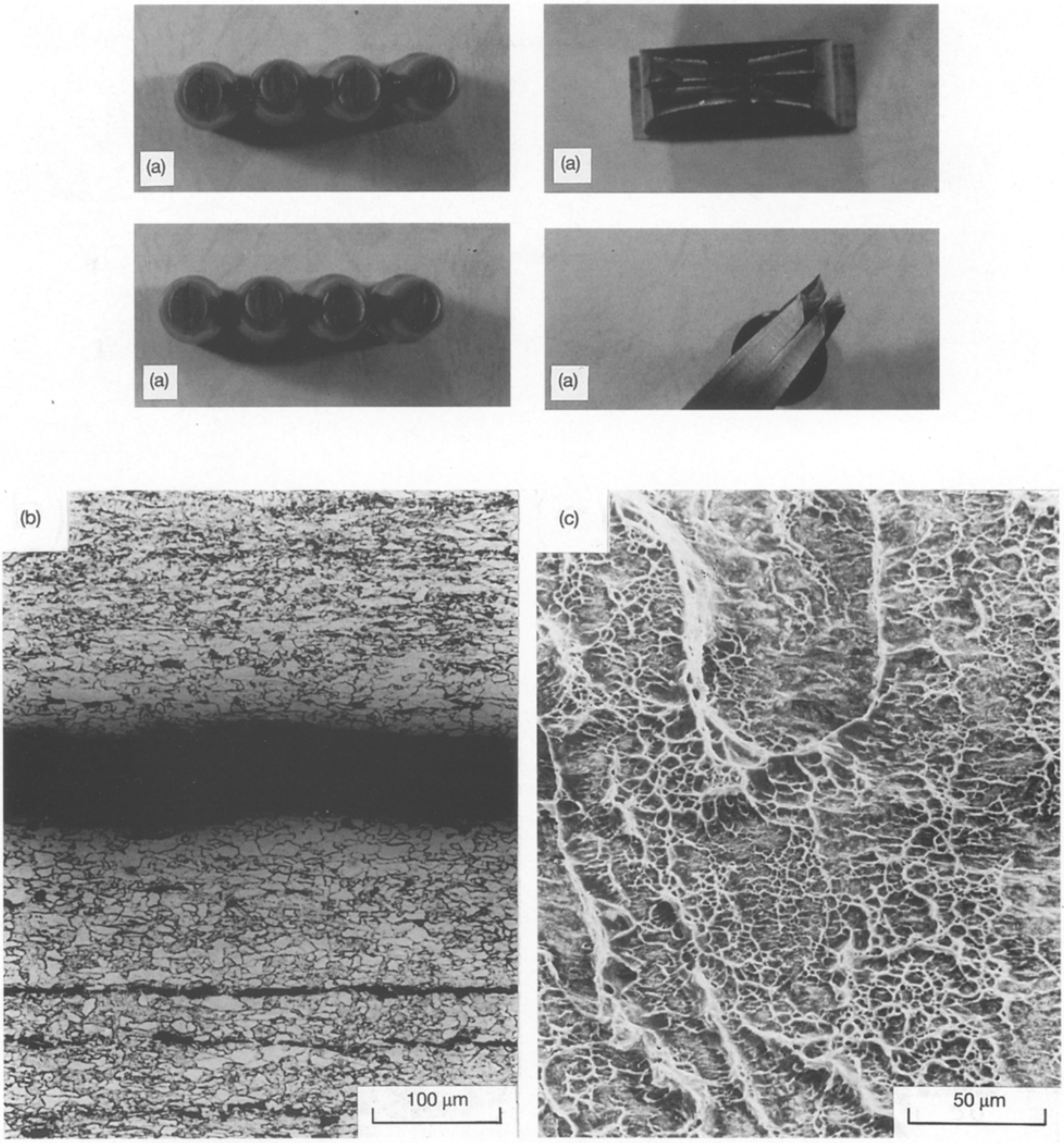

Figure 7 Photographs and micrographs showing the separation in the fractured tensile specimens: (a) photographs of the fractured specimens, (b) a micrograph of the propagation of the crack, and (c) a SEM micrograph of the fracture morphology of a specimen.

important to evaluate the HIC sensitivity of this boron ineffective zone. Fig. 8 shows a cross-section of the microstructure at the boron ineffective zone and the sound region of the ULCB steel after immersion in the BP solution for 96 h. It can be seen that the HIC is relatively more serious in the boron ineffective zone. Once the HIC has been initiated, it has a propensity to propagate along this region. In contrast, the HIC sensitivity is much lower in the sound region; some small HIC can occasionally be found. However, the propagation of this HIC in this region is significantly limited. This result indicates that the existence of the boron ineffective zone is deleterious to the HIC resistance of steels.

3.3. Propagation of cold cracking at the heat-affected zone

In the case of welding with a low heat input, it is quite easy to induce cold cracking at the heat-affected zone. In general, there are three factors which affect the heat-affected-zone cold-cracking sensitivity, that is, the microstructure, the hydrogen content, and the residual stress at the heat-affected zone. These factors usually have a synergistic effect on each other [15, 16]. In this study, it was found that the resistance to cold cracking of ULCB steels is excellent because of their extremely low carbon content. However, propagation of cold cracking along the boron ineffective zone has been found. Fig. 9 shows the microstructure of a cold

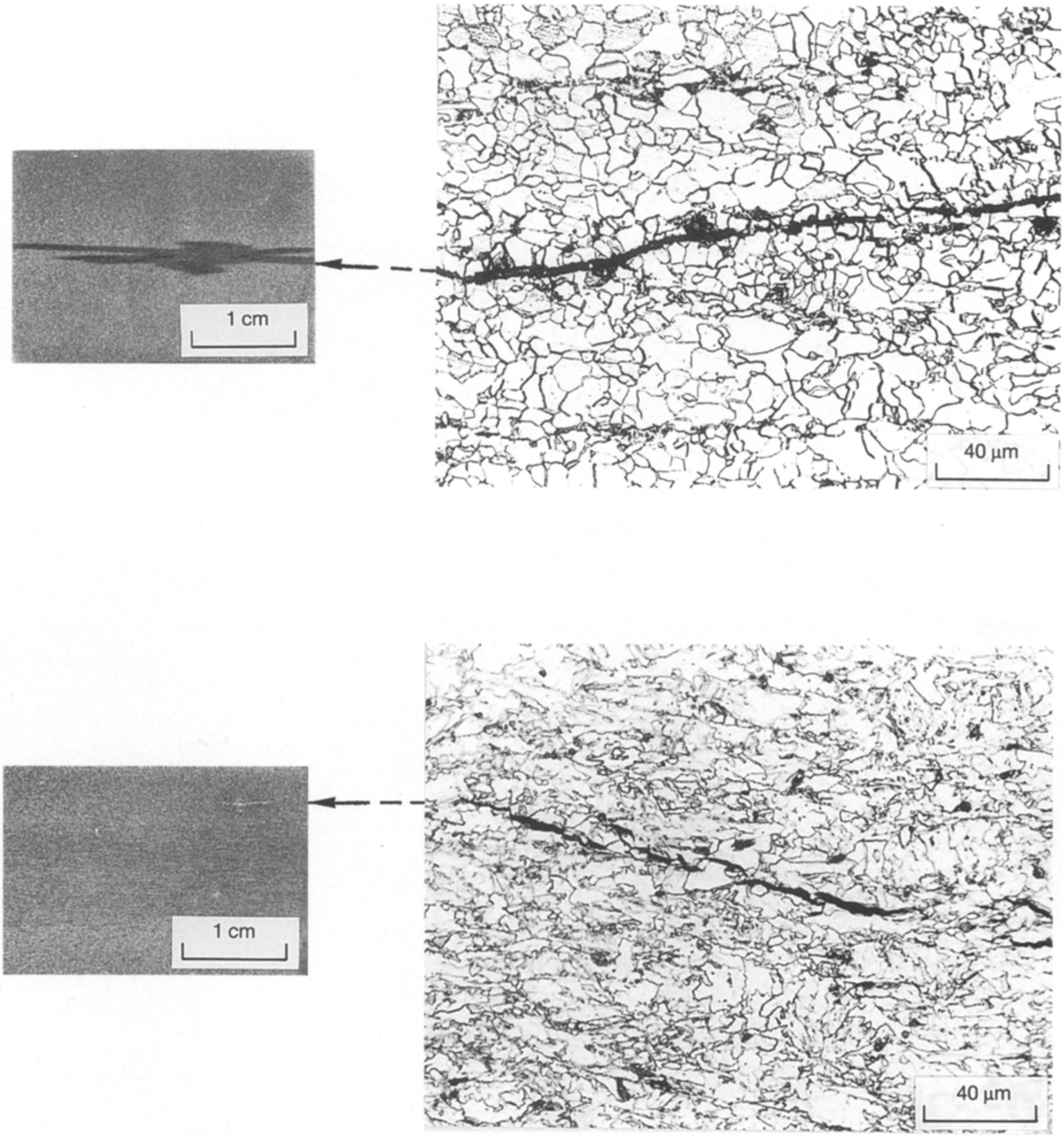

Figure 8 Photographs and micrographs of a cross-section of the microstructure of the ULCB steels after immersion in a BP solution for 96 h: (a) the boron ineffective zone, and (b) the sound, boron effective region.

crack found in a Y-grooved test specimen. The cold crack originates in the root of weld, and then it propagates toward the boron inffective zone. Normally, once the cold cracking initiates at the root of weld, it will propagate toward either the heat-affected zone or the weld metal [17]. The crack propagation along the base metal which was observed in this study has rarely been reported. The following mechanism for this abnormal-welding cold-cracking propagation is proposed. Because the strength of the boron inffective zone is much lower than that of the surrounding sound region, excessive plastic deformation will accumulate at this soft region under the action of the welding residual stress. When the accumulated strain exceeds the fracture strain of this material, the crack is induced in this excessively deformed soft region.

4. Conclusions

In the development of ULCB steels in CSC, a small, stringer-like, boron ineffective zone was found at the centre of the steel plate. From EPMA and boron autoradiograph analysis, it was found that the formation of the boron ineffective zone was due to the centre-line segregation of inclusions which strongly combined with boron and formed a boron-free zone in its vicinity. The microstructure of the boron ineffective zone was a conventional ferrite with a strength which was much lower than that of the surrounding bainite. The effects of this boron ineffective zone on the properties of steel have been evaluated and can be concluded to be as follows.

1. Separation will occur during tensile testing because of the existence of a soft boron ineffective zone. The occurrence of the separation does not have

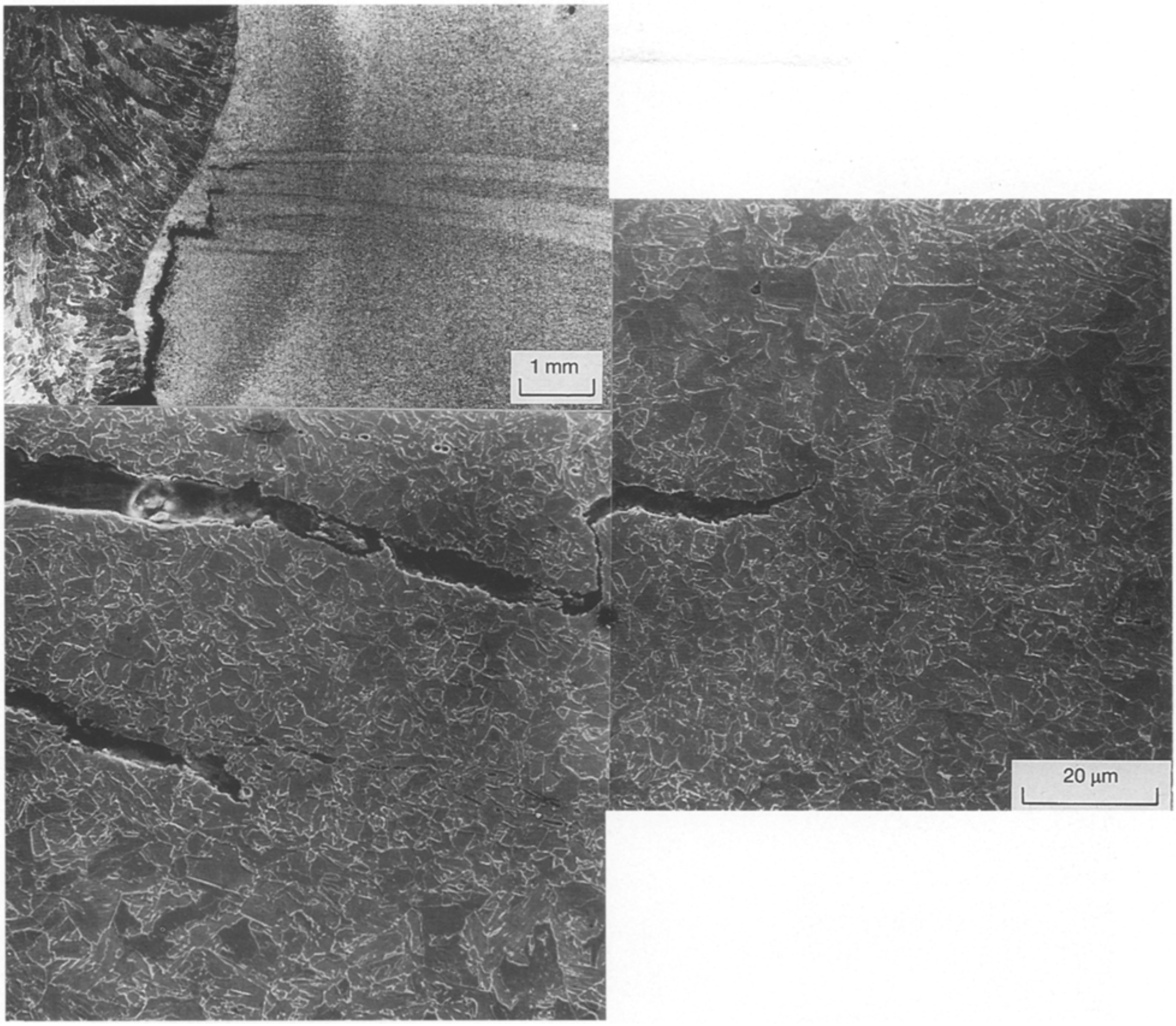

Figure 9 The microstructure of a cold cracking found in the Y-grooved-test specimen, showing the cold cracking which originated from the root of weld and then propagated towards the boron ineffective zone.

a significantly detrimental effect on the strength and toughness of steel plates, except that it reduces the elongation a little.

2. Since the pearlite band is easily observed in the boron ineffective zone, which is also the segregation zone of inclusions, the local aggravation of the hydrogen-induced cracks will take place at this region.

3. Due to the relatively soft ferrite–pearlite structure which forms at this boron ineffective zone, excess plastic deformation will accumulate at this region under the action of the welding residual stress; consequently, the cold cracking will propagate toward this boron ineffective zone.

References

1. A. P. COLDREN, Y. E. SMITH and R. L. CRYDERMAN, Proceedings of an AIME Symposium on Processing and the Properties of Low Carbon Steel (Cleveland, 1972) p. 163.
2. C. I. GRACIA and A. J. DEARDO, "Microalloyed HSLA steels" (ASM International, Chicago, 1988) p. 291.
3. B. M. KAPADIA, R. M. BROWN and W. J. MURPHY, *Trans. AIME* **242** (1968) 1687.
4. P. MAITREPIERRE, D. THIVELLIER and J. ROFES-VESNIS, "Hardenability concepts with applications to steel" (1978) p. 421.
5. M. SAEKI, M. F. KUROSAWA and M. MATSUO, *Trans. ISIJ*. **26** (1986) 1017.
6. M. TANINO, M. S. FUNAKI, H. KOMOTSU and Y. Q. ZHANG, *ibid.* **21** (1981) 231.
7. J. M. OBLAK and R. F. HEHEMANN, "Microalloyed HSLA steel" (American Society for Metals, Chicago, IL, 1988) p. 69.
8. V. BISS and R. L. CRYDERMAN, *Metall. Trans.* **2** (1971) 2267.
9. S. DIONNE, M. R. KRISHNADEV, L. E. COLLINS and J.D. BOYD, "Accelerated cooling of rolled steels" (American Institute of Mining, Metallurgical and Petroleum Engineers, Winnipeg, 1987) p. 71.
10. L. E. COLLINS, J. D. BOYD, J. A. JACKMAN and L. D. BAYLEY, "Microalloyed HSLA steels" (American Society for Metals, Chicago, 1988) p. 607.
11. T. YUTORI and R. OGAWA, in "International Conference on Steel Rolling", The Iron & Steel Institute of Japan, Tokyo, 1980, p. 992.
12. D. L. BOURELL, *Met. Trans A* **14** (1983) 2487.
13. Y. NAKAI, H. KURAHASHI, T. EMI and O. HAIDA, *Trans. ISIJ* **19** (1979) 401.
14. E. M. MOORE and J. J. WARGA, *Materials performance* **15** (1976) 17.
15. J. M. SAWHILL and T. WEDA, *Welding J.* **54** (1975) 1s.
16. P. J. BOOTHBY, *Metal Construction* **8** (1985) 508R.
17. M. INAGAKI, Y. ITO and Y. KOMIZO, IIW, Doc IX1412-86, (International Institute of Welding) 7 (1986).

Received 21 January 1993
and accepted 16 May 1994